C−H Bond Dissociation Energies of Alkyl Amines: Radical Structures and Stabilization Energies[§]

D. D. M. Wayner,[†] K. B. Clark,[†] A. Rauk,*,[‡] D. Yu,[‡] and D. A. Armstrong[‡]

Contribution from the Steacie Institute of Molecular Sciences, National Research Council of Canada, 100 Sussex Drive, Ottawa, Ontario K1A 0R6, Canada, and Department of Chemistry, The University of Calgary, Calgary, Alberta T2N 1N4, Canada

Abstract: A previous experimental study of the $^\alpha$C−H bond dissociation energies (BDEs) of amines indicated a significant decrease in BDE (or increase in radical stabilization energy, E_s) in the series primary, secondary, and tertiary. However, this was not supported by theoretical investigations. The $^\alpha$C−H BDEs of trimethylamine ((CH_3)$_3$-NH), triethylamine ((C_2H_5)$_3$NH), and tri-*n*-butylamine ((C_4H_9)$_3$NH) and of the cyclic secondary amines piperidine, piperazine, morpholine, and pyrrolidine were therefore determined by photoacoustic calorimetry in benzene solvent. Ab initio procedures, which incorporated isodesmic reactions to minimize residual correlation errors, were used to obtain the BDEs of several of these for direct comparisons. Also the BDEs of methylamine (CH_3NH_2), ethylamine ($C_2H_5NH_2$), isopropylamine ((CH_3)$_2$CHNH$_2$)), and dimethylamine ((CH_3)$_2$NH) were calculated as a check on the earlier results. The experimental BDEs in kJ mol^{-1} at 298 K ($\pm$10 kJ mol^{-1}), estimated from the photoacoustic calorimetric measurements, were as follows: trimethylamine 372, triethylamine 381, tri-*n*-butylamine 381, piperidine 385, piperazine 385, morpholine 389, and pyrrolidine 377. The ab initio results were in excellent agreement with these values. From earlier work and the present calculations the α-to-N C−H BDE of methylamine was estimated to be 388 $\pm$ <10 kJ mol^{-1}, corresponding to a radical stabilization energy, E_s, of ~51 kJ mol^{-1}. Contrary to the previous experimental finding, both theory and experiment showed that the increase in E_s on alkylation either at N or C is expected to be less than 4 kJ mol^{-1}. Values of $\Delta_f H^\circ_{298}$ for the α-C radicals of the smaller aliphatic amines, except that of methylamine, must therefore be revised. The three-electron two-orbital π-like interaction, which causes the $^\alpha$C radical stabilization, is maximized when the singly occupied sp^n orbital of C and the nonbonded doubly occupied sp^n orbital of N are anticoplanar to each other. Alkylamines preferably adopt a conformation in which at least one $^\alpha$C−H bond is anticoplanar to the lone pair on nitrogen, and the most stable carbon centered α-to-N free radical is that derived by abstraction of this H atom. In the five-membered pyrrolidine ring the radical adopts an envelope conformation with the C^5 carbon atom at the vertex. This accommodates the favorable alignment of the sp^n orbitals of C$^\bullet$ and N but has no C−H eclipsing interactions like those which occur in the parent. Thus, in effect, there is a reduction of strain on formation of the radical, and the BDE is lowered by ~8 kJ mol^{-1} below that of typical secondary amines.

Introduction

The effect of neighboring groups on C−H bond dissociation energies has been a subject of interest for many years.[1] The bond dissociation energy (BDE) in a compound (R−H) is defined by the equation

$$BDE(R-H) = \Delta_f H^\circ(R^\bullet) + \Delta_f H^\circ(H^\bullet) - \Delta_f H^\circ(R-H) \quad (1)$$

and the quantity [BDE(CH_3−H) − BDE(R−H)] is commonly referred to as the stabilization energy, E_s, of the radical R$^\bullet$.[2] The accepted value of BDE(CH_3−H) is 439 kJ mol^{-1}.[3] Systematic studies of E_s made for many types of radicals have shown that the presence of lone pairs of electrons on atoms adjacent to the radical center (e.g., N and O) results in a significant increase in E_s. The reason for this can be understood

Chart 1

CH₃–NH₂   **CH₂–NH₂•**
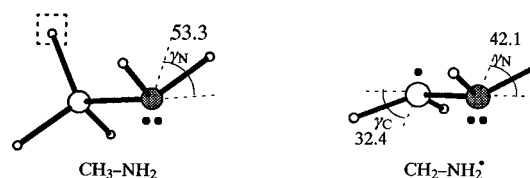
by reference to the structures of methylamine and the methyl-amine radical,[4] shown in Chart 1. The H atom opposite the lone pair of the nitrogen is the one that is lost and the anticoplaner arrangement of the semioccupied and lone pair orbitals permits the sharing of π electrons between the C and N centers. A radical structure of this form can be expected for all amines where the geometry is relatively unconstrained.

The C−H BDEs of $R^1R^2NCHR^3R^4$ amines and the E_s values of $R^1R^2NC^\bullet R^3R^4$ radicals (R^n = Me or H) were studied experimentally by Burkey et al.[5] Some of these species were investigated by ab initio methods (in some cases up to MP4) with the aid of isodesmic reactions.[6–10] The results are compared in Table 1. There is remarkably good agreement

[†] Steacie Institute.

[‡] University of Calgary.

[§] Keywords: amines; bond dissociation energies; radicals; stabilization energies; thermochemistry; radical structures.

[⊗] Abstract published in *Advance ACS Abstracts,* September 15, 1997.

(1) Dewar, M. J. S.; Fox, M. A.; Nelson, D. J. *J. Organomet. Chem.* **1980**, *185*, 157.

(2) BDE(R−H) and E_s are temperature dependent. The commonly used symbol for BDE at 0 K is D_0. At $T >$ 0 K BDE is a bond enthalpy, for which the symbol DH$_T$ may be used.

(3) Berkowitz, J.; Ellison, G. B.; Gutman, D. *J. Phys. Chem.* **1994**, *98*, 2744.

(4) Armstrong, D. A.; Rauk, A.; Yu, D. *J. Am. Chem. Soc.* **1993**, *115*, 666.

(5) (a) Griller, D.; Lossing, F. P. *J. Am. Chem. Soc.* **1981**, *103*, 1586. (b) Burkey, T. J.; Castelhano, A. L.; Griller, D.; Lossing, F. P. *J. Am. Chem. Soc.* **1983**, *105*, 4701.

(6) Goddard, J. D. *Can. J. Chem.* **1982**, *60*, 1250.

Table 1. Published BDEs of Amines and Radical Stabilization Energies[a]

amine	BDE(R−H)		E_s	
	expt[b]	calcd	expt[b]	calcd
H_2NCH_2H	393	396[c]	42	43,[d] 46[e]
$H_2NCH(CH_3)H$	377		59	
$H_2NC(CH_3)_2H$	372		63	39[f]
$CH_3N(H)CH_2H$	364		71	41[d]
$(CH_3)_2NCH_2H$	351		84	
	389[g]		50[g]	

[a] In kJ mol^{-1}. [b] Values from ref 5 quoted in kcal mol^{-1} to ± 2 kcal mol^{-1} with no specific indication of temperature. [c] Reference 9. [d] Reference 7. [e] Reference 8. [f] Reference 10. [g] See text.

between theory and experiment for methylamine.[11] However, the ab initio calculations do not reproduce the increases in E_s shown by experiment for isopropylamine and dimethylamine, and only Hartree−Fock level calculations are available for ethylamine and trimethylamine.[6] Further gas phase measurements of C−H BDEs of amines do not appear to have been reported since the publication of ref 5. However, a value of the C−H BDE for trimethylamine may be derived indirectly from the reduction potential of its radical cation. Thus $E_{(2)}^\circ$ for the half reaction

$$(CH_3)_2NCH_3^{\bullet+} + e^- = (CH_3)_2NCH_3 \qquad (2)$$
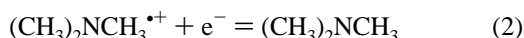
in aqueous solution has recently been found to be 1.04 V[12] and the C−H BDE can be calculated from that and the free energy change of reaction 3, which is known from the experimental pK_a

$$(CH_3)_2NCH_3^{\bullet+} = (CH_3)_2NCH_2^\bullet + H^+ \qquad (3)$$
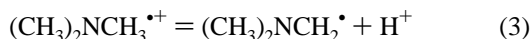
of 8.0.[13] The relation is shown in eq 4

$$E_{(2)}^\circ = \{D_{C-H} + T\delta S_{(5)}^\circ - \Delta G_{(3)}^\circ - \Delta_f H^\circ(H_{(g)}^\bullet)\}/F \quad (4)$$

where F is the Faraday constant, $\Delta S_{(5)}^\circ$ refers to the entropy change in reaction 5

$$(CH_3)_2NCH_2^\bullet{}_{(g)} + {}^1/_2 H_{2(g)} = (CH_3)_2NCH_{3(g)} \qquad (5)$$
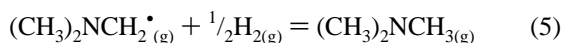
and the solution free energies of the amine and its radical are taken as identical. It may be noted that eq 4 was originally used in the reverse direction to calculate $E_{(2)}^\circ = 0.65$ V from the C−H BDE in Table 1.[4] With the new value of $E_{(2)}^\circ$, it yields 389 kJ mol^{-1} for D_{C-H} of trimethylamine and from this E_s is 50 kJ mol^{-1}.

Like the theoretical results in Table 1, the BDE of trimethylamine calculated from $E_{(2)}^\circ$ supports the view that E_s does not change significantly on the addition of further hydrocarbon groups on the nitrogen of the amine. It throws doubt on the experimental results of ref 5 and has prompted us to carry out further studies by both experiment and theory to resolve these apparent discrepancies. BDEs were determined by photoacoustic calorimetry for trimethylamine (Tma), triethylamine (Tea),

(7) Pasto, D. J.; Krasnansky, R.; Zercher, C. *J. Org. Chem.* **1987**, *52*, 3062.

(8) Lehd, M.; Jensen, F. *J. Org. Chem.* **1991**, *56*, 884.

(9) Leroy, G.; Sana, M.; Wilante, C. *J. Mol. Struct. (Theochem.)* **1991**, *228*, 37.

(10) Lein, M. H.; Hopkinson, A. C. *J. Comput. Chem.* **1985**, *6*, 274.

(11) There are some inconsequential (∼3 kJ mol^{-1}) discrepancies in E_s, which arise from slightly different values of D_{C-H} of CH$_4$ used by different authors and which we did not try to correct. In the remainder of this paper we have used the value of 439 kJ mol^{-1} from ref 3.

(12) Merenyi, G.; Lind, J. To be published.

and tri-*n*-butylamine (Tnba) and for the cyclic secondary amines piperidine (Ppd), piperazine (Ppz), morpholine (Mor), and pyrrolidine (Pyr). The BDEs of Tma, Ppd, Ppz, Mor, and Pyr were calculated by high level ab initio procedures for direct comparisons. Also the BDEs of methylamine (Ma), ethylamine (Ea), isopropylamine (Ipa), and dimethylamine (Dma) were calculated as a check on the earlier results in Table 1.

Experimental Methods

Materials. All solvents were of spectroscopic quality and used as received unless otherwise noted. The amines (Aldrich) were distilled prior to use. Ferrocene (Aldrich) was sublimed prior to use. Di-*tert*-butyl peroxide (Aldrich) was passed over activated alumina prior to use.

Photoacoustic Calorimetry. The calorimetry cell consists of a standard fluorescence cuvette (Hellma 221), modified to allow for continuous flow. After deoxygenation by purging with argon, the solutions were photolyzed using 8 ns pulses from a Laser Photonics Model VSL 337ND nitrogen laser (337.1 nm, 354.8 kJ mol^{-1}). The resulting shock wave was detected by a piezo electric transducer (Panametrics Model V101) in contact with the bottom of the cell (a thin layer of vacuum grease ensured good acoustic transmission). The signals were amplified (Panametrics Model 5670 ultrasonic preamp) and digitized (Tektronix Model TD20 Digital Oscilloscope). The signal-to-noise ratio was improved by signal averaging. Fluctuations in the laser energy were monitored using a L-PED pyroelectric device to which 10% of the incident laser beam was directed. The remaining radiation was passed through a 1 mm pinhole. The average laser energy in these experiments was < 20 mJ/pulse (i.e., flux < 6 mJ/cm^2). The solution transmission was measured using a second laser energy meter placed behind the cuvette. The instrument was calibrated using ferrocene in solutions that contained all of the components in the solvent of interest except the peroxide.

Experimental Results

The Photoacoustic Calorimetry (PAC) Technique. This involves measurement of the volume change when a brief pulse of irradiation from a laser strikes a solution containing reactants that initiate a predetermined, chemical change. The volume change produces a shock wave which is recorded by a sensitive microphone attached to the reaction vessel. The laser pulse-induced volume change can be converted to an enthalpic change, ΔH_{obs}, provided the thermoelastic properties of the solvent are known (i.e., the heat capacity, C_p°, and the thermal expansion coefficient, β). This is a comparative method in which a known amount of energy absorbed by the system induces a chemical transformation with the residual energy being returned to the system as heat. The measured volume consists of two components: that which is due to the thermal expansion and that which is due to a volume change on going from reactants to products. The former is the quantity required for bond energy determinations. The latter is generally significant only when the number of chemical species changes; i.e., when the number of bonds broken is not the same as the number of bonds formed.

The magnitude of the observed acoustic signal, S_{obs} is most simply expressed by eq 6 in which f^{obs} is the fraction of photon energy released as heat, $E_{h\nu}$ is the photon energy, OD is the optical density at the laser wavelength, and χ_s is the adiabatic expansion coefficient of the solvent (the parameters for which are given in eq 7 in which β is the thermal expansion coefficient, MW is the molecular weight of the solvent, ρ the density, and C_p° is the heat capacity). The constant c is determined by the geometry of the cell and a number of other instrument parameters. The observed volume change can be expressed as eq 8 where f^{th} is the fraction of the photon energy actually converted into heat and ΔV_{chem} is the volume change associated with the overall reaction.

$$S_{obs} = cf^{obs}E_{h\nu}(1 - 10^{-OD})\chi_s \quad (6)$$

$$\chi_s = \frac{\beta \cdot MW}{\rho C_p^\circ} \quad (7)$$

$$f^{obs} \cdot h\nu \cdot \chi_s = f^{th} \cdot h\nu \cdot \chi_s + \Delta V_{chem} \quad (8)$$

The relationship between f^{th} and the reaction enthalpy, ΔH_r, and the volume of reaction, ΔV_r are given by eqs 9 and 10, respectively. In both cases, the observed values must be corrected for the photochemical quantum yield of the reaction, Φ_r, since not every absorbed photon will lead to product formation.[14]

$$\Delta H_r = \frac{E_{h\nu}}{\Phi_r(1 - f^{th})} \quad (9)$$

$$\Delta V_r = \frac{\Delta V_{chem}}{\Phi_r} \quad (10)$$

Measurement of BDE(R−H)$_{sol}$ by PAC involves the irradiation of a solution containing the amine and di-*tert*-butyl peroxide with pulses from a nitrogen laser (337 nm, pulse width ~8 ns, up to 50 mJ/pulse) which produces *tert*-butoxyl radicals within 8 ns (eq 11). Subsequently, the *tert*-butoxyl radicals abstract *a*-CH hydrogen atoms from the amine. There is a kinetic requirement that the heat is evolved on a time scale which is much faster than the intrinsic response of the detector, i.e., k[amine] > 1×10^7 s^{-1}. Rate constants for the amines were determined by laser flash photolysis.

$$Me_3COOCMe_3 \xrightarrow{h\nu} 2Me_3CO^\bullet \quad (11)$$

$$Me_3CO^\bullet + RH \xrightarrow{k} Me_3COH + R^\bullet \quad (12)$$
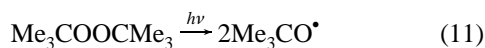
If all of the kinetic criteria are met, the acoustic signal will contain information proportional to ΔH_r and ΔV_r for the *overall* reaction shown in eq 13. These signals contain contributions from the energy of the laser pulse (337 nm, 354.8 kJ mol^{-1}), the bond energy of the O−O bond (eq 9), and the enthalpy for the exothermic hydrogen atom abstraction (eq 12).

$$Me_3COOCMe_3 + 2RH \rightarrow 2Me_3COH + 2R^\bullet \quad (13)$$
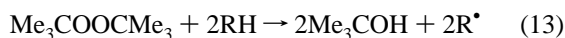
A relative experimental method is employed in which the photoacoustic signal generated in the reaction vessel, S_{obs}, is recorded as a function of the number of 337 nm photons absorbed by the sample, $(1 - 10^{-OD})$. The magnitude of $(1 - 10^{-OD})$ is altered by carrying out experiments using different concentrations of peroxide. A plot of S_{obs} vs $(1 - 10^{-OD})$ then yields an excellent straight line ($r \geq 0.996$) with a slope a_{obs}. Under the same experimental conditions the microphone response is calibrated using ferrocene which absorbs at 337 nm and converts *all* the absorbed energy to heat. A plot of the photoacoustic signal from the standard S_{st} vs $(1 - 10^{-OD})$ yields a second linear correlation with a slope a_{st}. The fraction of the photon energy converted to heat, f^{obs}, which is required (eq 8) is given by eq 14.

$$f^{obs} = \frac{a_{obs}}{a_{st}} \quad (14)$$

Finally, the bond energies are determined from an empirically derived correction term that takes both ΔV_r and changes in solvation energies between reactants and products into account. This approach has been described in detail elsewhere.[14] Provided there is not significant hydrogen bonding between the solvent and either RH or R$^\bullet$, a reasonable approximation of the gas phase BDE can be made. For benzene (the solvent used in all of these measurements), the BDE is given by eq 15, where $\Delta H_{corr} = 18.8$ kJ mol^{-1}.

$$BDE(R−H)_{gas} = \frac{\Delta H_{obs}}{2} + \Delta H_{corr} + 360.2 \text{ kJ mol}^{-1} \quad (15)$$

The C−H bond BDE of each RH species determined here at 298 K, together with data from the literature is given in Table 4. The largest source of error in the PAC determinations is in the determination of the ratio of slopes, f^{obs}, in eq 14. Although two very straight lines are obtained (i.e., $r \geq 0.9996$ or the run is discarded) an error of 1−2% in this slope leads to and error of 3−6 kJ/mol in the BDE. This leads to a relative error, ΔBDE, for values in Table 4 of ±6 kJ/mol on average. Of course this refers only to the experimental precision as the errors in the thermodynamic values used to derive eq 15 have not been included. Thus, the error in the accuracy of the determination is estimated to be ±10 kJ/mol, i.e., about twice the experimental precision.

Theoretical Calculations

Computational Details. All ab initio calculations presented here were performed with the Gaussian-94 molecular orbital packages.[15] The geometry optimizations were carried out at the HF/6-31G(D) and MP2/6-31G(D) levels. Vibrational frequencies were calculated at the HF/6-31G(D) level. For Ma, Dma, Tma, Ea, Ipa, and Pyr and their radicals the correlation corrections were estimated at the G2(MP2) level. The G2(MP2) procedure[16] includes a geometry optimization with the standard Hartree−Fock method and the 6-31G(D) split-valence basis set (HF/6-31G/(D)); a vibrational frequency calculation at the HF optimized geometry; MP2/6-31G(D) geometry optimization; two single-point post-HF calculations, i.e., QCISD(T)/6-311G(D,P) and MP2/6-311 + G(3DF,2P), on the MP2 optimized geometry in order to obtain an accurate estimate of the correlation energy. For the larger systems Ppd, Ppz, and Mor the G2(MP2)′ procedure, described in ref 17 was employed. In this the QCISD(T) and corresponding MP2 calculations were carried out with the smaller 6-31G(D,P) basis set, rather than the 6-311G(D,P) basis set of the standard G2(MP2) method. In all cases the vibrational frequencies calculated at the HF/6-31G-(D) level were scaled by a factor of 0.8929 in considering the zero-point energy.[18]

The C−H bond BDE of each RH species was calculated directly from the heat of reaction 16, given by $[E(RH) − E(R^\bullet)$

(13) Das, S.; Von Sonntag, C. *Z. Naturforsch.* **1986**, *41b*, 505.

(14) Wayner, D. D. M.; Lusztyk, E.; Page, D.; Ingold, K. U.; Mulder, P.; Laarhoven, L. J. J.; Aldrich, H. S. *J. Am. Chem. Soc.* **1995**, *117*, 8737.

(15) Frisch, M. J.; Trucks, G. W.; Schlegel, H. B.; Gill, P. M. W.; Johnson, B. G.; Robb, M. A.; Cheeseman, J. R.; Keith, T. A.; Petersson, G. A.; Montgomery, J. A.; Raghavachari, K.; Al-Laham, M. A.; Zakrewski, V. G.; Ortiz, J. V.; Foresman, J. B.; Cioslowski, J.; Stefanov, B. B.; Nanayakkara, A.; Challacombe, M.; Peng, C. Y.; Ayala, P. Y.; Chen, W.; Wong, M. W.; Andres, J. L.; Replogle, E. S.; Gomperts, R.; Martin, R. L.; Fox, D. J.; Binkley, J. S.; Defrees, D. J.; Baker, J.; Stewart, J. P.; Head-Gordon, M.; Gonzalez, C.; Pople, J. A. *Gaussian 94, (SGI-Revision B.3)*; Gaussian, Inc.: Pittsburgh, PA, 1995.

(16) Curtiss, L. A.; Raghavachari, K.; Pople, J. A. *J. Chem. Phys.* **1993**, *98*, 1293.

(17) Armstrong, D. A.; Yu, D.; Rauk, A. *Can. J. Chem.* **1996**, *74*, 1192.

(18) Pople, J. A.; Schlegel, H. B.; Krishnan, R.; Defrees, D. J.; Binkley, J. B.; Frisch, M. J.; Whiteside, R. A.; Hout, R. F.; Hehre, W. J. *Int. J. Quantum Chem. Symp.* **1981**, *15*, 269.

$- E(\text{H}^\bullet)]$, where the E's are the G2(MP2) energies. In order to obtain

$$\text{RH} = \text{R}^\bullet + \text{H}^\bullet \qquad (16)$$

BDEs at 298 K, values of $H^\circ_{298} - H^\circ_0$ were required for each species. These quantities were calculated by standard statistical thermodynamic methods based on the rigid rotor-harmonic oscillator model[19] and using the frequencies obtained at HF/6-31G(D) level. Again the frequencies were scaled by a factor of 0.8929 in these calculations.

As a means of reducing residual errors due to basis set and correlation effects, BDEs can also be derived from the heats of isodesmic reactions.[20] In the context of BDEs, these reactions can be represented by process 17

$$\text{X}^\bullet + \text{RH} = \text{XH} + \text{R}^\bullet \qquad (17)$$
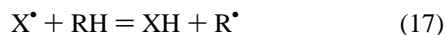
in which XH is a reference molecule for which the BDE, $D_{\text{C-H}}(\text{XH})$, is known accurately from experiment. The heat of reaction, $\Delta H_{(17)}$, is evaluated from the ab initio energies, and $D_{\text{C-H}}(\text{R-H})$ is then given by

$$D_{\text{C-H}}(\text{R-H}) = D_{\text{C-H}}(\text{XH}) + \Delta H_{(17)} \qquad (18)$$

In effect, the error in the calculated BDE of XH serves as a correction for the BDE of RH. The highest accuracy (greatest cancellation of residual errors) would be achieved if R and X are as similar as possible and the level of the theoretical method is as high as possible. In the present instance CH_3OH was used as a reference, since, due to lone pairs on the oxygen, the $^\bullet\text{CH}_2\text{OH}$ radical exhibits stabilization analogous to the amines. The C-H BDE of this molecule has recently been examined by several researchers.[3,21,22] Here the mean of the values recommended in these three recent publications (395.0 kJ mol^{-1} at 0 K; 401.7 kJ mol^{-1} at 298 K) was used.

Results

Acyclic Amines and Pyrrolidine. The equilibrium structures of Ma, Dma, Tma, Ea, Ipa, and Pyr and their radicals were obtained from a straightforward application of the G2(MP2) procedures. The acyclic radicals all have anticoplanar structures similar to that shown for $\text{H}_2\text{NCH}_2^\bullet$ in Chart 1. Calculations for some of these species have been reported elsewhere (for example, $(\text{CH}_3)_2\text{NCH}_2^\bullet$, and $(\text{CH}_3)_3\text{N}$ were studied in ref 4). The structures are not therefore presented here. Each of the acyclic parent amines has a pyramidal N atom with angles within a few degrees of the tetrahedral angle, 109.5, and a staggered arrangement of bonds at the methyl groups attached to N (Chart 1). One $^\alpha$C-H bond of the methyl group is anticoplanar to the nonbonding orbital accommodating the N lone pair. In the case of isopropylamine, the most stable (by 1.4 kJ mol^{-1}) C-N rotational conformation also has the $^\alpha$C-H bond anticoplanar to the N lone pair. For ethylamine, the two conformations are within 0.03 kJ mol^{-1} of each other.

The five-membered ring heterocycle, pyrrolidine (Figure 1), exists in an envelope conformation with the N atom out of the plane of the four C atoms (an N^1 envelope) and the N-H bond in a pseudoequatorial orientation. This conformation also has an $^\alpha$C-H bond anticoplanar to the N lone pair but eclipsed β methylene groups. In the radical, the five-membered ring adopts
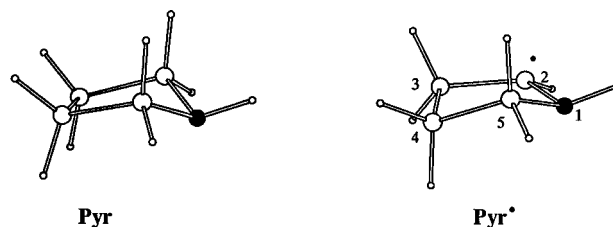
(19) McQuarrie, D. A. *Statistical thermodynamics*; Harper & Row: 1973.
(20) Hehre, W. J.; Ditchfield, R.; Radom, L.; Pople, J. A. *J. Am. Chem. Soc.* **1970**, *92*, 4796.
(21) Dobe, S.; Berces, T.; Turanyi, T.; Marta, F.; Grussdorf, J.; Temps, F.; Wagner, H. Gg. *J. Phys. Chem.* **1996**, *100*, 19864.
(22) Johnson, R. D. III; Hudgens, J. W. *J. Phys. Chem.* **1996**, *100*, 19874.

Figure 1. Structures of pyrrolidine (Pyr) and its alpha to N radical (Pyr$^\bullet$). Pyr has C_s symmetry; Pyr$^\bullet$ has C_1 symmetry. The filled circle is N; large and small open circles are C and H, respectively.

Table 2. Total Energies (Hartree), $H^\circ_{298} - H^\circ_0$ (kJ mol^{-1}) and Calculated α-C-H BDEs (kJ mol^{-1}) of Methylamine, Dimethylamine, Trimethylamine, Isopropylamine, and Pyrolidine Species

			α-C-H BDEs		
amine species	total energy	$H^\circ_{298} - H^\circ_0$	G2(MP2)[a] (0 K)	ISO[b] (0 K)	ISO[c] (298 K)
$\text{H}_2\text{N CH}_3$	−95.66452	11.5	389.7	382.0	388
$\text{H}_2\text{N CH}_2^\bullet$	−95.01609	11.5			
$\text{CH}_3\text{HN CH}_3$	−134.87957	14.2	387.6	379.9	386
$\text{CH}_3\text{HN CH}_2^\bullet$	−134.23195	14.4			
$(\text{CH}_3)_2\text{N CH}_3$	−174.09996	17.2	388.0	380.3	387
$(\text{CH}_3)_2\text{N CH}_2^\bullet$	−173.45217	17.5			
$\text{H}_2\text{N CH}_2\text{CH}_3$	−134.89137	14.3	385.6	377.9	384
$\text{H}_2\text{N CHCH}_3^\bullet$	−134.24451	14.6			
$\text{H}_2\text{N CH(CH}_3)_2$	−174.12141	17.4	387.8	380.1	388
$\text{H}_2\text{N C(CH}_3)_2^\bullet$	−173.47370	19.5			
Pyr	−212.14288	15.3	380.2	372.5	379
Pyr$^\bullet$	−211.49808	15.2			
HO CH_3	−115.53181	11.41[d]	402.7	395.0[e]	
$\text{HO CH}_2^\bullet$	−114.87843	11.24[d]			

[a] From G2(MP2) energies of RH, R$^\bullet$, and H$^\bullet$. [b] Based on the isodesmic reaction: $\text{HOCH}_2^\bullet + \text{XH} = \text{X} + \text{HOCH}_3$. [c] Corrected to 298 K using the above $H^\circ_{298} - H^\circ_0$ data and 6.2 kJ mol^{-1} for H$^\bullet$ from ref 23. [d] From ref 22. [e] Experimental value from ref 3.

a different slightly distorted envelope conformation to accommodate the favorable alignment of the sp^n orbitals of C$^\bullet$ and N, and all of the C-H bonds in the radical are moderately staggered with respect to each other and the N-H bond, Figure 1. Thus, in this C^5 envelope conformation with the C^5 carbon atom at the vertex, there are no C-H eclipsing interactions like those which occur in the Pyr parent. The resulting "relief of strain" in the radical appears to affect the BDE (see below).

The total energies calculated at the G2(MP2) level are given in Table 2, along with the calculated values of $H^\circ_{298} - H^\circ_0$ and the C-H BDEs at 0 K based on $\Delta H_{(16)}$ and $\Delta H_{(17)}$ under the headings G2(MP2) and ISO, respectively. The ISO BDEs at 298 K in the last column were obtained for comparison with experimental results. They have been rounded off to the nearest kJ mol^{-1}. The comparison with the experimental BDEs is made in Table 4. It may be noted from column three in Table 2 that $H^\circ_{298} - H^\circ_0$ values for the parent and radical species are usually within 1 kJ mol^{-1}, which means that the only significant term in the thermal correction comes from $H^\circ_{298} - H^\circ_0$ of H$^\bullet$, which is 6.2 kJ mol^{-1}.[23]

The Six-Membered Ring Cyclic Amines. The procedures employed to obtain the radical structures for the larger cyclic Ppd, Ppz, and Mor systems were more complex than for the above smaller species. For the parent compounds, only the "chair" structures, which are known to be more stable than the "boat" forms, were considered. For each cyclic amine these were obtained first. Then computations on the radicals were initiated by removing H atoms from axial or equatorial positions and allowing the new structure to optimize. Often the same radical was produced from both starting points. The equilibrium geometries are outlined in Figure 2, and details of the structures

Table 3. Total Energies (E), ZPEs, Relative Energies (ΔE) and Calculated BDEs for Piperidine, Piperazine, and Morpholine

amine species	HF/6-31G*			MP2(full)/6-31G*		G2(MP2)′		BDE ISO at 298 K (kJ mol^{-1})
	E (hartree)	ZPE (kJ mol^{-1})	ΔE (kJ mol^{-1})	E (hartree)	ΔE (kJ mol^{-1})	E (hartree)	BDE (kJ mol^{-1})	
Ppd								
-e (C_s)	-250.188 71	449.2	0	-251.030 88	0	-251.370 64		
-a (C_s)	-250.187 41	448.8	3	-251.029 92	2			
-e•	-249.567 27	410.7	0	-250.385 20	0	-250.723 80	385.5	384
-a•	-249.557 25	407.1	23	-250.372 30	31			
Ppz								
-ee (C_{2h})	-266.168 96	419.5	0	-267.039 50	0	-267.401 94		
-ae (C_s)	-266.167 62	419.0	3	-267.038 59	2			
-aa (C_{2h})	-266.165 74	418.5	8	-267.037 21	5			
-ae•	-265.539 29	377.3	14	-266.392 80	0	-266.755 12	385.5	384
-ee•	-265.545 70	380.7	0	-266.391 74	6	-266.753 06	390.9	389
-b•	-265.537 45	378.7	20	-266.383 95	25			
-ea•	-265.535 43	377.1	24	-266.378 42	38			
Mor								
-e (C_s)	-285.997 72	384.1	0	-286.879 43	0	-287.266 88		
-a (C_s)	-285.995 72	383.5	5	-286.878 00	3			
-e(N)•	-285.368 13	342.0	3	-286.232 17	0	-286.619 39	387.2	385
-a(O)•	-285.369 71	344.8	1	-286.226 68	17	-286.612 37	405.7	404
-e(O)•	-285.370 26	345.0	0	-286.226 24	18			
-b(O)•	-285.363 34	343.4	17	-286.219 46	35			
H•	-0.498 23	0.0		-0.498 23		-0.500 00		
HOCH$_2$•						-115.529 91		
HOCH$_3$						-114.876 40	403.0	

Table 4. C−H BDEs and E_s Values in kJ mol^{-1} at 298 K (Recommended Values in Boldface)[a]

Amine	Radical Structure	BDE(Calc.)[b]	E_s(Calc)	BDE(Expt.)	E_s(Rec.)
Primary:					
Ma	H$_2$NC•H$_2$	**388**	51	393[c]	**51**
Ea	H$_2$NC•HCH$_3$	**384** 385[d]	55	377[c]	**55**
Ipa	H$_2$NC•(CH$_3$)$_2$	**388**	51	372[c]	**51**
Secondary:					
Dma	CH$_3$NHC•H$_2$	**386**	53	364[c]	**53**
Ppd		384[d]	55	**385**	**54**
Ppz		384[d]	55	**385**	**54**
Mor		385[d]	54	**389**	**50**
Pyr		379	60	**377**	**62**
Tertiary:					
Tma	(CH$_3$)$_2$NC•H$_2$	**387**	52	372 351[c] 389[e]	**52**
Tea	(CH$_3$CH$_2$)$_2$NC•HCH$_3$	–	–	**381**	**58**
Tnba	(n-C$_4$H$_9$)$_2$NC•H(n-C$_3$H$_7$)	–	–	**381**	**58**

[a] From this study, unless stated otherwise. Recommended values have an uncertainty of ±10 kJ mol^{-1}. [b] At G2(MP2) level, unless otherwise stated. [c] Values from ref 5 quoted in kcal mol^{-1} to ±2 kcal mol^{-1} with no specific indication of temperature. [d] At G2(MP2)′ level. [e] Calculated from ref 12, see text.

may be obtained from the authors. In the following text species are described by the parent symbol, followed by "-a" or "-e" to indicate whether the N−H bond(s) are axial or equatorial. As usual, a superscript dot indicates a radical. Examples would be Ppz-ee for the parent piperazine with equatorial−equatorial geometry (i.e., both N−H bonds equatorial) and Ppd−a• for the piperidine radical α to the N−H with axial geometry (Figure 2). For morpholine, the radical sites α to O were investigated as well as α to N. They are distinguished by placing (O) and (N), respectively, before the dot, e.g., Mor-e(O)• and Mor-e(N)•. Finally, an α-to-N boat form radical of Ppz, Ppz-b•, and an

α-to-O boat form radical of Mor, Mor-b(O)•, were examined to determine their energies relative to the chair form radicals.

The energies of the parents and radicals at the HF/6-31G*, MP2(full)/6-31G*, and G2(MP2)′ levels are given in Table 3. Also listed are the ZPEs at HF/6-31G* and the energies relative to the lowest structure of each type (ΔE). The values of ΔE at the MP2(full)/6-31G* level have also been given in Figure 2, and the structures are presented with those of lowest energy nearest to the dividing line. Thus BDEs for thermally equilibrated species should correspond primarily to removal of an H from the parent structure immediately on the left of the line to form the radical structure immediately on the right.

While the differences are only a few kJ mol^{-1}, the results in Table 3 and Figure 2 show that the parent amines always have lower energy with the N−H's in equatorial geometries, as would be expected. This was also observed for the radicals, except for Ppz-ee• which has a higher energy than Ppz-ae•. As indicated in Table 3, Ppz-ee• was in fact lower than Ppz-ae• at the HF/6-31G* level. However, the relative energies for the MP2(full)/6-31G* calculation were confirmed at the still higher G2(MP2)′ level (Table 3). The α to N boat form radical Ppz-b• has a substantially higher energy than Ppz-ae• and Ppz-ee• (Figure 2 and Table 3). Likewise Mor-b(O)• has a significantly higher energy than Mor-e(O)• and Mor-a(O)•. Radicals in the boat geometry are not therefore likely to contribute significantly to thermally equilibrated populations and have not been considered further.

Intuitively in Mor one expects a greater stabilization in the α-to-N radicals than in the α-to-O radicals. That was not true at the HF/6-31G* level, where the Mor-e(O)• and Mor-a(O)• radicals were lower in energy than Mor-e(N)• (Table 3). However, the expected energy order was observed at the MP2-(full)/6-31G* level and maintained at the G2(MP2)′ level (Table 3 and Figure 2).

The G2(MP2)′ energies were also used to evaluate the BDEs from $\Delta H_{(16)}$ and the 0 K ISO BDEs from $\Delta H_{(17)}$. The latter are not shown, but the 298 K ISO BDEs in the last column of Table 3 were obtained from them by taking 6.2 kJ mol^{-1} for $H_{298}^{\circ} - H_0^{\circ}$ of H•[23] as above and assuming that the $H_{298}^{\circ} - H_0^{\circ}$ for the parent and radical species were the same. Based on the results for the smaller radicals in Table 2, this will not
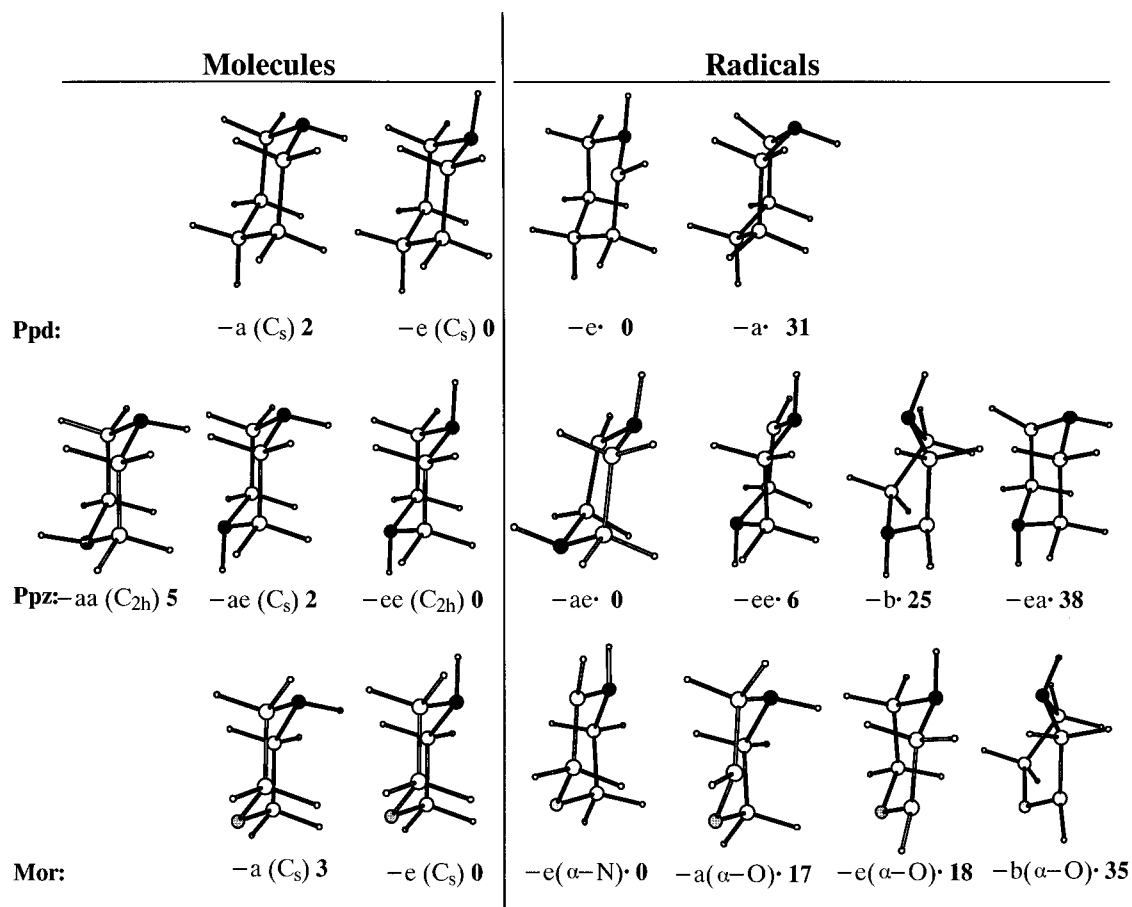
Molecules | **Radicals**

Ppd: −a (C$_s$) **2**   −e (C$_s$) **0** | −e• **0**   −a• **31**

Ppz:−aa (C$_{2h}$) **5**   −ae (C$_s$) **2**   −ee (C$_{2h}$) **0** | −ae• **0**   −ee• **6**   −b• **25**   −ea• **38**

Mor: −a (C$_s$) **3**   −e (C$_s$) **0** | −e(α−N)• **0**   −a(α−O)• **17**   −e(α−O)• **18**   −b(α−O)• **35**

Figure 2. Structures of piperidine (Ppd), piperazine (Ppz), and morpholine (Mor) molecules and radicals. The symmetries are C_1 unless stated otherwise. The numbers in boldface are relative energies in kJ/mol at the {MP2/6-31G*//MP2/6-31G* + 0.8929 ZPE(HF/6-31G*)} level with stablest species nearest to the dividing line. Atoms are as follows: N, filled circle; O, shaded circle; C, large open circle; H, small open circle; and the N−H is indicated as axial (a) or equatorial (e). For Mor, radical sites are alpha to N (α-N) or alpha to O (α-O).

introduce errors of more than 1 kJ mol^{-1}. The ISO BDEs at 298 K in Table 3 for the α-to-N radicals and the parents of lowest energy (384, 384, and 385 kJ mol^{-1}, respectively, for Ppd, Ppz, and Mor) are essentially identical. The BDE for formation of Ppz-ee• from Ppz is only a few kJ mol^{-1} larger, and this radical form may be present in thermal equilibrium with Ppz-ae•. The BDE for formation of the α-to-O radical in Mor, 404 kJ mol^{-1}, is significantly larger than 385 kJ mol^{-1} and similar to the experimental value for CH$_3$OH, 401.7 kJ mol^{-1}.[3,21,22]

The calculated ISO BDEs at 298 K are compared with the present experimental ones and with those from refs 5 and 12 in Table 4. Based on the discussion in the following section, "recommended" values have been selected for each amine, and these are in boldface. Values of the radical stabilization energies derived from the calculated, E_s(calc), and the recommended BDEs, E_s(rec), have also been given.

Discussion

A general consideration of the structures of the parents and radicals is presented first. Following this the theoretical basis for the stabilization of the radicals is discussed. The experimental and calculated BDEs are then compared and discussed.

Structures. Each of the acyclic parent amines has a pyramidal N atom with angles within a few degrees of the tetrahedral angle, 109.5, and a staggered arrangement of bonds at the methyl group(s) attached to N (Chart 1). One $^{\alpha}$C−H bond of the methyl group is anticoplanar to the nonbonding orbital accommodating the N lone pair. The most stable

structures of the six-membered ring cyclic amines are chair conformations with the N−H bonds occupying equatorial positions (Figure 2). These also have $^{\alpha}$C−H bonds anticoplanar to the N lone pair. The chair conformations with one N−H bond in an axial position are less stable by 2 kJ mol^{-1}. The conformation of piperazine with two axial N−H bonds is less stable than the diequatorial form by 5 kJ mol^{-1}. The five-membered ring heterocycle, pyrrolidine (Figure 1), exists in an envelope conformation with the N atom out of the plane of the four C atoms (an N^1 envelope) and the N−H bond in a pseudoequatorial orientation. This conformation also has an $^{\alpha}$C−H bond anticoplanar to the N lone pair but eclipsed β methylene groups. *In short, in all of the parent amines, there is a bias in favor of conformations with $^{\alpha}$C−H bonds anticoplanar to the N lone pair as in Chart 1.*

Each of the acyclic α-to-N radicals has a structure analogous to that shown in Chart 1. Both the $^{\alpha}$C and N atoms are flattened pyramids separated by r_{CN} = 1.40 ± 0.02 Å. The *anti* arrangement of the bonds is a consequence of the attractive three-electron π bonding which is maximized when the sp^n hybrid orbitals of the $^{\alpha}$C and N are anticoplanar, Figure 3. In the case of pyrrolidine (Figure 1), the five-membered ring adopts a different slightly distorted envelope conformation to accommodate the favorable alignment of the sp^n orbitals of C• and N. The required arrangement of bonds (or alternatively, the π-like orbitals) is also achievable without incursion of ring strain in the chair forms of the six-membered ring heterocycles (Figure 2). *Thus in every case, the most stable radical has the N−H*
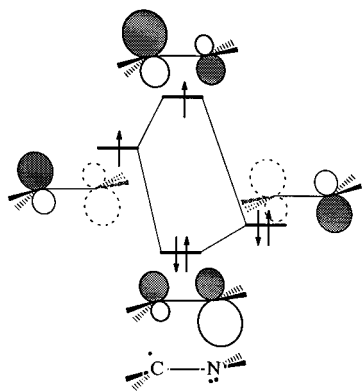
Figure 3. The two-orbital three-electron radical stabilizing interaction diagram.

and $^{\alpha}C^{\bullet}$−*H bonds in quasiequatorial positions*, *i.e.*, *with the N lone pair and singly occupied C orbitals in an anticoplanar orientation.*

The Basis for Stabilization. Stabilization of the $^{\alpha}C^{\bullet}$ radical site by lone pair electrons on N can be understood in terms of the simple two-orbital interactions shown in Figure 3. The *direction* of changes in BDEs or stabilization energies (E_s) expected for alkyl substitutions at C or N can be explained on a similar basis. Alkyl groups possess one local group orbital which can interact to stabilize a radical site in precisely the same way as is illustrated for the $-NH_2$ substituent in Figure 3. However, the stabilization by a methyl group at the radical site is expected to be less than by the amino group, because the doubly occupied methyl group orbital and the sp^n orbital of the $^{\alpha}C^{\bullet}$ site are further apart in energy. Thus, the present calculations indicate that the radical stabilization by a single amino nitrogen atom is 51 kJ mol^{-1} (for methylamine, Table 4), which is considerably greater than E_s for $-CH_3$ (16 kJ mol^{-1} derived from D_{C-H} for ethane[3]). The consequence of substitution by an alkyl group on the N is ambiguous due to opposing effects. The two-orbital four-electron interaction between the alkyl group orbital and the N lone pair has the effect of raising the N lone pair orbital closer to the energy of the $^{\alpha}C^{\bullet}$ orbital and therefore indirectly increasing the intrinsic interaction shown in the Figure 3. On the other hand, substitution on N also serves to "spread" the N lone pair, thereby reducing the coefficient of the sp^n orbital and *reducing* the intrinsic interaction. The cumulative effects on E_s arising from substitution by multiple alkyl groups at either $^{\alpha}C^{\bullet}$ or N are not expected to be additive but should be in the same direction. However, even if the prediction of the *direction* of the energy changes is unambiguous, simple arguments cannot predict the *magnitude*. For this, one must have recourse to experiment or more rigorous theory.

The present E_s of 55 kJ mol^{-1} in Table 4 for ethylamine suggests that the additional effect of a methyl group at the $^{\alpha}C^{\bullet}$ site in the presence of the amino group is only 4 kJ mol^{-1}, not 17 kJ mol^{-1} as indicated by the previous data of ref 5 (Table 1). The result for isopropyl amine ($E_s = 51$ kJ mol^{-1}) suggests that the second methyl group may actually be destabilizing by 4 kJ mol^{-1}. Single methyl substitution on N results in $E_s = 53$ kJ mol^{-1} (dimethylamine, Table 4). A second methyl group does not have an additional influence on E_s (52 kJ mol^{-1}, trimethylamine). The three six-membered ring heterocycles, which represent the single alkyl at C *plus* single alkyl at N substitution pattern, have E_s's of 55 kJ mol^{-1} (Ppd, Ppz) or 54 kJ mol^{-1} (Mor). In summary, the present ab initio calculations imply that E_s is *determined primarily* by the presence of the nitrogen atom. Additional alkyl substitution, either directly at $C^{\bullet}$ or indirectly at N, produces a maximum additional stabilization of 4 kJ mol^{-1}.

Comparison of Experimental and Calculated BDEs. The agreement between the present experimental and calculated values for the six-membered cyclic amines Ppd, PPz, Mor, and Pyr is surprisingly good, within 4 kJ mol^{-1} or less. Thus the experimental results strongly support the view that an E_s of ~55 kJ mol^{-1} is correct for the single alkyl at C *plus* single alkyl at N substitution pattern. Particularly interesting is the fact that theory and experiment both track the ~8 kJ mol^{-1} reduction in the BDE of Pyr (BDE = 377 kJ mol^{-1}(exptl) and 379 kJ mol^{-1}(calc); Table 4) below the BDEs of the six-membered rings. This is not attributed to electronic effects at the radical site but, as stated in the Results for the Theoretical Calculations above, to relief of the eclipsing repulsions at the β-methylene sites in the N^1 envelope conformation of the parent (Figure 1). A similar conclusion for five-membered ring systems was given in ref 24.

The agreement is rather poor for Tma, where the experimental value of 372 kJ mol^{-1} is 15 kJ mol^{-1} below the calculated. However, this result appears to be anomalous, since Tea and Tnba both exhibit BDEs of 381 kJ mol^{-1}, which is much closer to the 387 kJ mol^{-1} calculated value for Tma. At the same time, the calculated Tma result agrees well with the value of 389 derived in the Introduction from the data of refs 12 and 13. The value of 387 kJ mol^{-1} is recommended for that amine. Ab initio calculations were not done explicitly for Tea and Tnba. However, from the discussion above one can anticipate a ~4 kJ mol^{-1} reduction in BDE (increase in E_s) for the change from methyl to higher straight chain alkyl groups. Thus the BDEs for Tea and Tnba should be near 383 kJ mol^{-1}, which is close to the observed value of 381 kJ mol^{-1}.

The main conclusion from the new experimental results is that $^{\alpha}C-H$ BDEs for tertiary amines and the six-membered cyclic secondary amines are in the narrow range of 381−387 kJ mol^{-1}. Although the BDE of 393 kJ mol^{-1} obtained in ref 5 for methylamine is in agreement (within the ±10 kJ mol^{-1} uncertainty) with the present calculated value of 388 kJ mol^{-1}, the rather strong dependence of the BDE on alkyl substitutions at the $^{\alpha}C$ and N positions, shown by the data for Epa, Ipa, Dma, and Tma (see Table 4), is not supported by the present experimental results or the calculations. Thus it appears that the results of ref 5 are subject to a source of error which increases with size of the amine.

The significant increase in the BDEs of Ea, Ipa, Dma, and Tma above the values reported in ref 5 means that properties calculated from them must be changed. These include values of $\Delta_f H^{\circ}_{298}$ of the α-C radicals in refs 25 and 26 and amine reduction potentials in ref 4, all of which will also increase. Using $\Delta_f H^{\circ}_{298}$ of the parent compounds from ref 22 and the ab initio BDE values in Table 4, we estimate values of $\Delta_f H^{\circ}_{298}$ in kJ mol^{-1} for the α-C radicals as follows: Ea 119, Ipa 86, Dma 150, and Tma 145, all subject to an uncertainty of ±10 kJ mol^{-1}. The reduction potentials can be recalculated from these.[4]

Stabilization Energies and the Correction from the Isodesmic Reaction. The direct G2(MP2)-based calculation of the HOCH$_2$−H BDE at 0 K by eq 16 yields 402.7 kJ mol^{-1}, while the G2(MP2)′-based calculation gives 403.0 kJ mol^{-1}. The experimental value is 395.0 kJ mol^{-1} (see Theoretical Calculations). The differences of 7.7 and 8.0 kJ mol^{-1} at the G2(MP2) and G2(MP2)′ levels, respectively, are measures of the corrections needed to compensate for correlation errors in radicals of this kind. The use of CH$_3$OH as the isodesmic

(23) Wagman, D. D.; Evans, W. H.; Parker, V. B.; Schumm, R. H.; Halow, I.; Bailey, S. M.; Churney, K. L.; Nuttal, R. L. *J. Phys. Chem. Ref. Data* **1982**, *11*, Suppl. No. 2.
(24) Clark, K. B.; Wayner, D. D. M.; Demirdji, S. H.; Koch, T. H. *J. Am. Chem. Soc.* **1993**, *115*, 2447.

partner for the amines in reaction 17 is based on the premise that the OH in the $HOCH_2^•$ radical provides a mechanism of stabilization analogous to NH_2 in amine α-C radicals. In effect it results in systematic corrections of 7.7 and 8.0 kJ mol^{-1} to the 0 K BDEs of the radicals calculated at the G2(MP2) and G2(MP2)′ levels, respectively. The good agreement between the present experimental results and calculations for the cyclic amines supports the view that this correction was appropriate. In the earlier theoretical work of ref 9 ethane was used as an isodesmic partner. The CH_3 group in $CH_3CH_2^•$ radical does not provide a good π-bond mechanism of stabilization, and ethane is a less satisfactory partner in reaction 7. As a direct illustration, the $HOCH_2$−H 298 K BDE was calculated to be 405.8 kJ mol^{-1},[9] ∼4 kJ mol^{-1} higher than the experimental BDE used here. This difference in isodesmic partners accounts for the difference between the 298 K BDE of 388 kJ mol^{-1} calculated here for CH_3NH_2 (Table 4) and the value of 396 kJ mol^{-1} from ref 9 (Table 1). In the same vein, the values of E_s from the other earlier theoretical studies in Table 1 are less than those calculated from the present BDEs (see Table 4). The major reason for this is again the choice of the isodesmic partner in reaction 17, which in the earlier work was CH_4 or C_2H_6.[27] One may put these points in perspective by realizing that the E_s values for $CH_3^•$, $CH_3CH_2^•$, and $HOCH_2^•$ derived from experimental BDEs in ref 3 are respectively 0, 16, and 37 kJ mol^{-1}. Clearly the use of $HOCH_3$ should give the best cancellation of residual correlation errors for α-amino radicals.

As implied above, there is no indication that strain increases the BDE (reduces E_s) for any of the cyclic radicals of lowest energy. In fact, as indicated above, in the case of Pyr the reduction of strain in the radical acts to reduce the BDE. However, the cases of Ppd-a$^•$ and Ppz-ea$^•$ in Table 3 can be used to illustrate the point that E_s is significantly reduced for α-to-N radicals *without* the favorable alignment of the sp^n orbitals of C$^•$ and N (i.e., without both N−H and ^{α}C$^•$−H in

(25) Lias, S. G.; Bartmess, J. E.; Liebman, J. F.; Holmes, J. L.; Levin, R. D.; Mallard, W. G. Gas Phase Ion and Neutral Thermochemistry. *J. Phys. Chem. Ref. Data* **1988**, *17*, Suppl. No. 1.

(26) Stein, S. E.; Lias, S. G.; Liebman, J. F.; Levin, R. D.; Kafafi, S. A. *NIST Standard Reference Data Base 25*, *NIST Structures and Properties Version 2.0*; U.S. Department of Commerce Gaithersburg, MD, 1994.

(27) Another point is that thermal and ZPE differences were neglected in some of the earlier calculations, and this would contribute to differences from the present values.

quasi-equatorial positions, and the N lone pair and singly occupied C orbitals in an anticoplanar orientation, Figure 2). Usually, in the calculations the generation of a radical site by removal of either an equatorial H, or an axial H from the parent amine with an axial N−H bond, resulted in optimization by inversion of the C$^•$ and/or N site to give the most stable conformation. However, in the above two cases it was possible to locate α-to-N radicals *without* the favorable alignment. Those radicals were less stable than the corresponding optimum structures, Ppd-e$^•$ and Ppz-ae$^•$, by 31 and 38 kJ mol^{-1}, respectively (Table 3). These numbers provide a direct measure of the energetic consequences of the reduction in the three-electron π-like bonding.

Conclusions

Alkylamines preferably adopt a conformation in which at least one ^{α}C−H bond is anticoplanar to the lone pair on nitrogen. The most stable carbon centered α-to-N free radical is that derived by abstraction of this H atom. The α-to-N C−H BDE of methylamine is 388 kJ mol^{-1} with an expected uncertainty of less than 10 kJ mol^{-1}, corresponding to a radical stabilization energy, $E_s = 51$ kJ mol^{-1}. The stabilization is attributed to a three-electron two-orbital π-like interaction which is maximized when the singly occupied sp^n orbital of C and the nonbonded doubly occupied sp^n orbital of N are anticoplanar to each other. The increase in E_s on alkylation either at N or C is predicted to be less than 4 kJ mol^{-1}, contrary to the accepted literature. Values of $\Delta_f H°_{298}$ for the α-C radicals of the smaller aliphatic amines, except that of Ma, must therefore be revised.

The case of the five-membered pyrrolidine ring is interesting in that, to accommodate the favorable alignment of the sp^n orbitals of C$^•$ and N, the radical adopts an envelope conformation with the C^5 carbon atom at the vertex, and this conformation has no C−H eclipsing interactions like those which occur in the parent. Thus, in effect, there is a reduction of strain on formation of the radical, and the BDE is lowered by ∼8 kJ mol^{-1} below that of typical secondary amines.

JA971365V